ASME Design Automation Conference
September 1987, Boston, USA

DESIGN AND CONSTRUCTION OF A STATICALLY-BALANCED DIRECT DRIVE ARM

H. Kazerooni
S. Kim
Mechanical Engineering Department
111 Church St., SE
University of Minnesota
Minneapolis, MN 55455

ABSTRACT

A statically-balanced direct drive robot manipulator is being constructed at the University of Minnesota for analysis of manufacturing tasks such as deburring and grinding when Impedance Control (8,10,11) is used to control the robot. This mechanism using a four bar linkage is designed without extra counterweights. As a result of elimination of the gravity forces on the drive system, smaller actuators (and consequently smaller amplifiers) are chosen to guarantee the acceleration of about 5g without overheating the motors. This mechanism results in closed-form solution for inverse kinematics. The closed-form solutions for dynamic and inverse kinematic have been derived. High torque, low speed brush-less AC synchronous motors are used to power the robot. The relatively "large" workspace of this configuration is suitable for manufacturing tasks. Graphite epoxy composite material is being used for the construction of the robot links.

INTRODUCTION

A novel statically balanced direct drive arm, with a four bar link mechanism has been designed for compensation of some of the drawbacks of serial type(1,2) and parallelogram type (3,4) direct drive arms. Before describing the properties of this arm, some disadvantages and advantages of direct drive arms are discussed here:

1. Speed. The maneuvering speed of the direct drive arms is not necessarily greater than the non-direct drive arms. The maximum achievable speed for a given architecture depends on the transmission ratio. The optimal transmission ratio is a function of the inertia of the links. A simple example in the appendix shows that for a given architecture a non-direct drive arm can be faster than a direct drive arm.

2. Static Payload. It is obvious that for a given set of motors, direct drive arms have lower static payload than the non-direct drive arms. This is because of the inherent evident property of reducer transmission systems.

3. Overheating. Elimination of the transmission system causes the inertial force and the gravitational force of the links affect the motors. In other words, the motors "feel" the inertial and the gravitational forces without any reduction in size. The direct effect of the forces cause the motors to overheat in the direct drive arms. This overheating exists even in the static case when the arm is only under its static load, and gravity is the only dominant force in the system.

4. Backlash and Friction. The direct drive arms are free from mechanical backlash and friction due to elimination of transmission systems. A small mechanical backlash in the transmission system causes the gear teeth to wear faster. The high rate of wear in the gear develops even larger backlash. About 25% of the torque in non-direct drive arms are used to overcome

the friction(6).

5. Structural Stiffness. The structural stiffness of the direct drive arms are greater than the non-direct drive systems. About 80 % of the total mechanical compliance in most non-direct drive industrial robots are caused by transmission systems(7,16). The high structural stiffness allows for wide bandwidth control. The low structural stiffness of non-direct drive arms due to existence of many mechanical elements in the transmission system, is a limiting factor on achievement of a relatively wide bandwidth control system.(10,11,12)

6. Performance and Control. Because of elimination of the transmission systems, and consequently backlash, the control and performance analysis of direct drive arms are more straightforward than the non-direct (drive arms not necessarily "easier").

7. Accuracy. The accuracy of direct drive arms is questionable. The lack of the transmission system eliminates cogging, backlash, and its corresponding limit cycle in the control system. On the other hand the motor vibrations in the direct drive systems are directly transferred to the robot end point.

This paper presents the work on the design of a self balanced direct drive arm with a four bar linkage. The architecture of this arm is such that the gravity term is completely eliminated from the dynamic equations. This balanced mechanism is designed without adding any extra counterbalance weights. The new features of this new design are as follows:

I. Since the motors never get affected by gravity, the static load will be zero and no overheating results in the system in static case.

II. Because of the elimination of the gravity terms, smaller motors with less stall torque (and consequently smaller amplifiers) can be chosen for a desired acceleration.

III. Because of the lack of gravity terms, higher accuracy can be achieved. This is true because the links have steady deflection due to constant gravity effect. This will give better accuracy and repeatability for fine manipulation tasks.

IV. As depicted in Figure 2, the architecture of this robot allows for a "large" work-space. The work-space of this robot is quite attractive from the stand point of manufacturing tasks such as assembly and deburring.

MOTIVATION

The following scenario reveals the crucial needs for adaptive electronic compliance control (Impedance Control)(8,10,11) in manufacturing. Consider an assembly operation by a human worker. There are some parts on the table to be assembled. Each time that the worker decides to reach the table and pick a part, she/he always encounters the table with non-zero speed. The worker assembles the parts with a non-zero speed also. The ability of the human hand in encountering an unknown and unstructured environment(9,17), with non-zero speed, allows for a higher speed of operation. This ability in human beings flags the existence of a compliance control mechanism in biological systems that guarantees the "controllability" of contact forces in constrained maneuvering, in addition to high speed maneuvering in unconstrained environment. With the existing state of technology we do not have an integrated sensory robotic assembly system that can encounter an unstructured environment as a human worker can. No existing robotic assembly system is faster than a human hand. The compliancy in the human hand allows the worker to encounter the environment with non-zero speed. The above example does not imply that we choose to imitate human being factory level physiological/psychological behavior as our model to develop an overall control systems for manufacturing tasks such as assembly and finishing processes. We stated this example to show 1) A reliable and optimum solution for simple manufacturing tasks such as assembly does not exist; 2) the existence of an efficient, fast compliance control system in human beings that allows for superior and faster performance. We believe that Impedance Control is one of the key issues in development of high speed manufacturing operations. A direct drive robot arm is being constructed at the University of Minnesota to investigate high speed manufacturing tasks (in particular deburring and grinding) under Impedance Control methodology.

ARCHITECTURE

Figure 1 shows the schematic diagram of the University of Minnesota direct drive arm. The arm has three degrees of freedom, all of which are articulated drive joints. Motor 1 powers the system about a vertical axis. Motor 2 pitches the entire four bar linkage while motor 3 is used to power the four bar linkage. Link 2 is directly connected to the shaft of motor 2. Figure 2 shows the top view and side view of the robot. The coordinate frame $X_iY_iZ_i$ has been assigned to link i of the robot for i=1,2,..,5. The center of coordinate frame $X_1Y_1Z_1$ corresponding to link 1 is located at point 0 as shown in figure 2. The center of the inertial global coordinate frame $X_0Y_0Z_0$ is also located at point 0 (The global coordinate frame is not shown in the figures). The joint angles are represented by θ_1, θ_2, and θ_3. θ_1 represents the rotation of link 1; coordinate frame $X_1Y_1Z_1$ coincides on global coordinate frame $X_0Y_0Z_0$ when $\theta_1 = 0$. θ_2 represents the pitch angle of the four bar linkage as shown in figure 2. θ_3 represents the angle between link 2 and link 3. Shown are the conditions under which the gravity terms are eliminated from the dynamic equations.

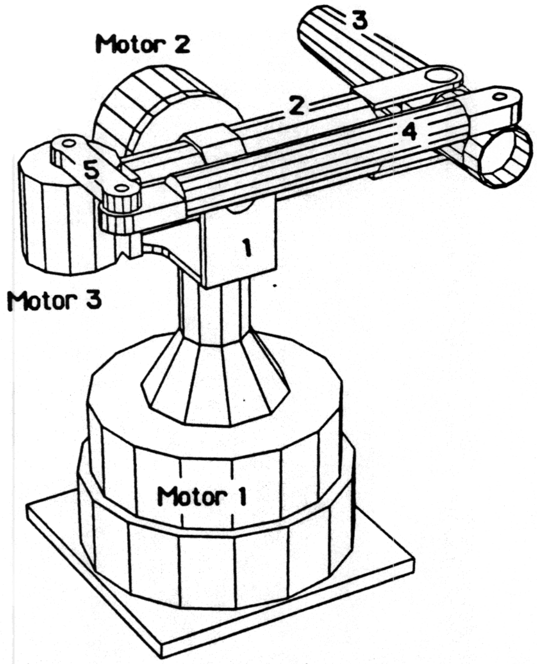

Figure 1: University of Minnesota Direct Drive Arm

Figure 3 shows the four bar linkage with assigned coordinate frames. By inspection the conditions under which the vector of gravity passes through origin, 0, for all possible values of θ_1 and θ_3 are given by equations 1 and 2.

$$[\ m_3\bar{x}_3 - m_4L_5 - m_5\bar{x}_5 \quad \sin\theta_3 = 0 \tag{1}$$

$$g\ (mt_3 + m_5) - m_2\bar{x}_2 - m_3(L_2 - g) - m_4(\bar{x}_4 - g\ ) - [\ m_3\bar{x}_3 - m_4L_5 - m_5\bar{x}_5\ ]\ \cos\theta_3 = 0 \tag{2}$$

where:

m_i = mass of each link,

L_i = length of each link,

$\bar{x}_i$ = the distance of center of mass from the origin of each coordinate frame,

mt_3 = mass of motor 3.

Conditions 1 and 2 result in:

$$m_3\bar{x}_3 - m_4L_5 - m_5\bar{x}_5 = 0 \tag{3}$$

$$g\ (mt_3 + m_5) - m_2\bar{x}_2 - m_3(L_2 - g) - m_4(\ \bar{x}_4 - g\ ) = 0 \tag{4}$$

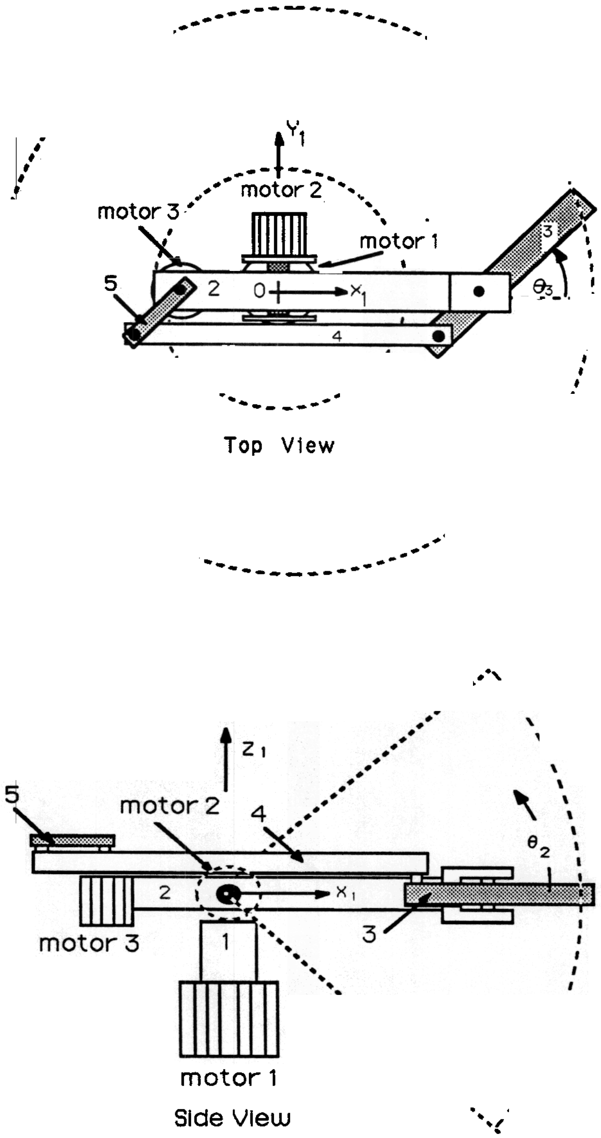

Figure 2: The Side View and Top View of the Robot

If equations 3 and 4 are satisfied, then the center of gravity of the four bar linkage passes through point 0 for all the possible configurations of the arm. Note that the gravity force still passes through 0 even if the plane of the four bar linkage is tilted by motor 2 for all values of θ_2.

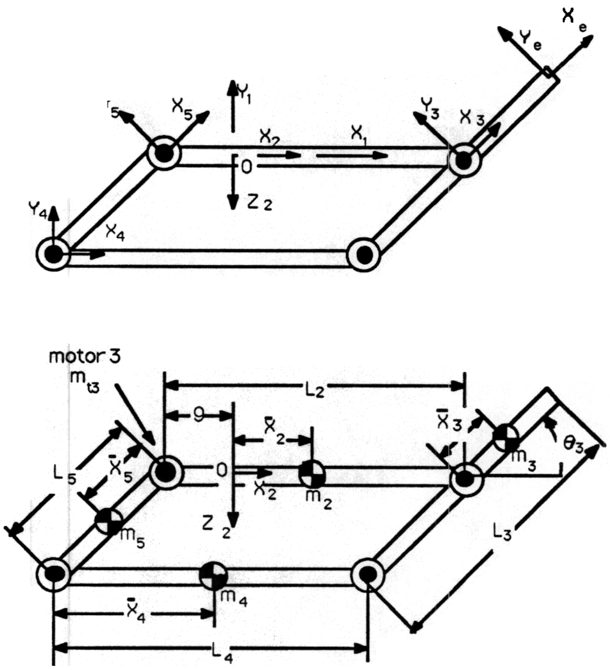

Figure 3: Four Bar Link Mechanism

FORWARD KINEMATICS

The forward kinematic problem is to compute the position of the end point in the global coordinate frame $X_0Y_0Z_0$, given the joint angles, θ_1, θ_2, and θ_3. The joint coordinate relationship of i coordinate frame relative to i-1 coordinate frame in figure 4 can be represented by the homogeneous transformation matrix ${}^{i-1}T_i$ that follows the modified Denavit-Hartenberg notation. (6)

$$
{}^{i-1}T_i = \begin{pmatrix} C\theta_i & -S\theta_i & 0 & a_{i-1} \\ S\theta_i C\alpha_{i-1} & C\theta_i C\alpha_{i-1} & -S\alpha_{i-1} & -S\alpha_{i-1} d_i \\ S\theta_i S\alpha_{i-1} & C\theta_i S\alpha_{i-1} & C\alpha_{i-1} & C\alpha_{i-1} d_i \\ 0 & 0 & 0 & \end{pmatrix} \tag{5}
$$

S and C refer to Sine and Cosine functions, and a_i, d_i, α_i and θ_i are link parameters. The link parameters of the arm are listed in table 1. Note that the coordinate frame $X_1Y_1Z_1$ coincides with the global coordinate frame, $X_0Y_0Z_0$, when θ_1 is zero.

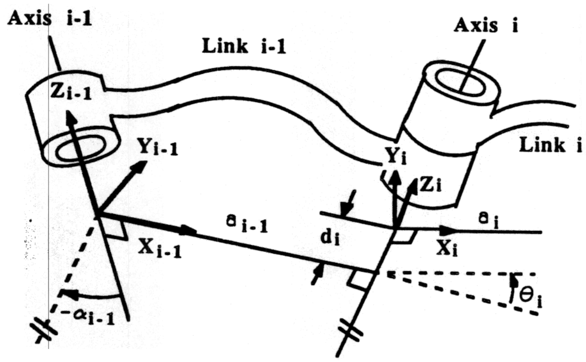

a_i = the distance from Z_i to Z_{i+1} measured along X_i;
α_i = the angle between Z_i and Z_{i+1} measured about X_i;
d_i = the distance from X_{i-1} to X_i measured along Z_i;
θ_i = the angle between X_{i-1} and X_i measured about Z_i;

Figure 4: Link Coordinates and Parameters

Table 1: Link parameters

Frame i	α_{i-1}	a_{i-1}	d_i	θ_i
$X_1Y_1Z_1$	0	0	0	θ_1
$X_2Y_2Z_2$	90°	0	0	θ_2
$X_3Y_3Z_3$	- 90°	$L_2 - g$	0	θ_3
$X_eY_eZ_e$	0	$L_3 - L_5$	0	0

Assume end point coordinate frame $X_eY_eZ_e$ has the same orientation as coordinate frame $X_3Y_3Z_3$

The homogeneous transformation matrix, which describes the position and orientation of coordinate frame $X_eY_eZ_e$ with respect to the global coordinate frame $X_0Y_0Z_0$ is given by

$$
{}^{0}T_e = \begin{pmatrix} C & -C_1C_2S_3 - S_1C_3 & -C_1S_2 & (C_1C_2C_3 - S_1S_3)(L_3-L_5) + C_1C_2(L_2 - g) \\ S_1C_2C_3 + C_1S_3 & -S_1C_2S_3 + C_1C_3 & -S_1S_2 & (S_1C_2C_3 + C_1S_3)(L_3-L_5) + S_1C_2(L_2 - g) \\ S_2C_3 & -S_2S_3 & C_2 & S_2(L_2 - g) + S_2C_3(L_3 - L_5 \\ 0 & 0 & 0 & \end{pmatrix} \tag{6}
$$

where S_i = Sin (θ_i), and C_i - Cos (θ_i)

INVERSE KINEMATICS

The inverse kinematic problem is to calculate the joint angles for a given end point position with respect to global coordinate frame. The closed-form of inverse kinematics of the proposed arm derived using the standard method(6,15). The end point position of the robot relative to the global coordinate frame is characterized by P_x, P_y, and p_z. The joint angles for the given end point position can be determined using the following equations

$$\theta_1 - \text{atan2}(P_y, P_x) - \text{atan2}\left((L_3 - L_5)\sin\theta_3, \pm\sqrt{P_x^2 + P_y^2 - (L_3 - L_5)^2 \sin^2\theta_3}\right) \quad (7)$$

$$\theta_2 - \sin^{-1} \frac{P_z}{(L_2 - g) + (L_3 - L_5 \cos\theta_3} \quad (8)$$

$$\theta_3 - \cos^{-1} \frac{P_x^2 + P_y^2 + P_z^2 - (L_2 - g)^2 - (L_3 - L_5)^2}{2(L_2 - g)(L_3 - L_5} \quad (9)$$

DYNAMICS

The closed-form dynamic equations have been derived for the purpose of controller design. The dynamic behavior of the arm can be presented by the following equation (5,6)

$$M(\theta)\ddot{\theta} + CE(\theta)(\dot{\theta}^2) + CO(\theta)(\dot{\theta}\dot{\theta}) + G(\theta) - \tau \quad (10)$$

Where:

$\tau - (\tau_1\ \tau_2\ \tau_3)^T$	3×1 vector of the motor torques,
$M(\theta)$	3×3 position dependent symmetric positive definite inertia matrix,
$CE(\theta)$	3×3 centrifugal coefficients matrix,
$CO(\theta)$	3×3 Coriolis coefficients matrix,
$G(\theta)$	3×1 vector of gravity force,

$\ddot{\theta} - (\ddot{\theta}_1\ \ddot{\theta}_2\ \ddot{\theta}_3)^T$

$(\dot{\theta}\dot{\theta}) = \dot{\theta}_1\dot{\theta}_2\quad \dot{\theta}_1\dot{\theta}_3\quad \dot{\theta}_2\dot{\theta}_3)^T$

$(\dot{\theta}^2) = \dot{\theta}_1^2\quad \dot{\theta}_2^2\quad \dot{\theta}_3^2)^T$

$$M(\theta) - \begin{pmatrix} M_{11} & M_{12} & M_{13} \\ M_{12} & M_{22} & 0 \\ M_{13} & 0 & M_{33} \end{pmatrix} \qquad CE(\theta) - \begin{pmatrix} 0 & CE_{12} & CE_{13} \\ CE_{21} & 0 & 0 \\ CE_{31} & CE_{32} & 0 \end{pmatrix}$$

$$CO(\theta) - \begin{pmatrix} CO_{11} & CO_{12} & CO_{13} \\ 0 & CO_{22} & CO_{23} \\ CO_{31} & 0 & 0 \end{pmatrix} \qquad G(\theta) - \begin{matrix} 0 \\ 0 \\ 0 \end{matrix}$$

where

$M_{11} - I_1 + C_2^2(I33 + I_{z3} + I55 + 2C_3I35 + I_{y2} + M_2\overline{x}_2^2) + S_2^2(S_3^2\, I33 + I_{y3}) + C_3^2\, I_{x3} + I_{x2})$

$M_{12} - S_2S_3(I35 + C_3(I33 + I_{y3} - I_{x3}))$

$M_{13} - C_2(I33 + I_{z3} + C_3I35)$

$M_{22} - I_{z2} + M_2\overline{x}_2^2 + C_3^2(I33 + I_{y3}) + S_3^2I_{x3} + I55 + 2C_3I35$

$M_{33} - I33 + I_{z3}$

$CE_{12} - C_2S_3(I35 + C_3(I33 + I_{y3} - I_{x3}))$

$CE_{13} - - C_2S_3I35$

$CE_{21} - S_2C_2(I_{y2} - I_{x2} + M_2\overline{x}_2^2 - S_3^2I_{y3} + C_3^2(I33 - I_{x3}) + I55 + I_{z3} + 2C_3I35)$

$CE_{31} - S_3(C_2^2I35 - S_2^2C_3(I33 + I_{y3} - I_{x3}))$

$CE_{32} - S_3(I35 + C_3(I33 + I_{y3} - I_{x3}))$

$CO_{11} - - 2CE_{21}$

$CO_{12} - - 2CE_{31}$

$CO_{13} - - S_2(2S_3^2I33 + I_{z3} + \cos2\theta_3(I_{x3} - I_{y3}))$

$CO_{22} - S_2(2C_3^2I33 + I_{z3} + 2C_3I35 - \cos2\theta_3(I_{x3} - I_{y3}))$

$CO_{23} - - 2CE_{32}$

$CO_{31} - - S_2(I33 + \cos2\theta_3(I33 + I_{y3} - I_{x3}) + I_{z3} + 2C_3I35)$

where

$I33 - m_3\overline{x}_3^2 + m_4L_5^2 + m_5\overline{x}_5^2$

$I55 - m_3(L_2 - g)^2 + m_4(\overline{x}_4 - g)^2 + m_5 g^2$

$I35 - m_3\overline{x}_3(L_2 - g) - m_4(\overline{x}_4 - g)L_5 + m_5\overline{x}_5 g$

$M_2 - mt_3 + m_2$

I_{xi}, I_{yi}, and I_{zi} are the mass moments of inertia relative to x, y, z axis at the center of mass of a link i. The gravity term, $G(\theta)$ becomes zero when equations 3, 4 are satisfied in the arm. This condition holds for all possible configurations.

MOTOR AND THE CAD SOFTWARE

Since at low speeds, AC torque motors do not tend to cog, low speed, high torque, and brush-less AC synchronous motors are chosen to power the robot. Each motor consists of a ring shaped stator and a ring shaped permanent magnet rotor with a large number of poles. The rotor is made of rare earth magnetic material (Neodymium) bonded to a low carbon steel yoke with structural adhesive. The stator of the motor (with winding) is fixed to the housing for heat dissipation.

A CAD software has been developed for dynamic analysis and motor selection. The motors are selected such that they guarantee 5g acceleration in the "worst case" maneuvering for the arm of a reach of over 70.4 cm. Figure 5 shows an example of the output of the CAD software. In this example, the robot is moved from the initial point $\theta = (0° \; -30° \; 45°)$ to the final position of $\theta = (124° \; 32° \; 107°)$ with $\ddot{\theta}_1 = 52(1-4t)$ rad/sec^2, $\ddot{\theta}_2 = 26(1-4t)$ rad/sec^2 and $\ddot{\theta}_3 = 26(1-4t)$ rad/sec^2.

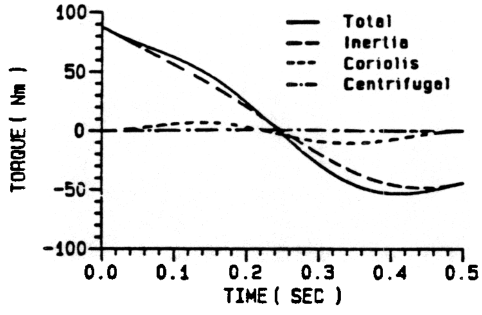

Motor for Joint

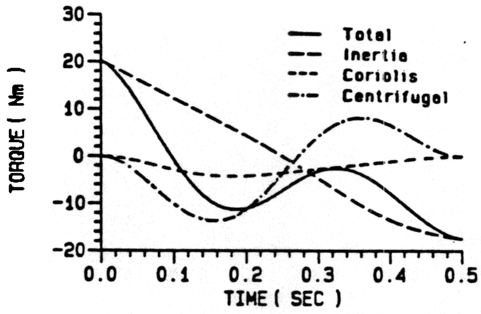

Motor for Joint 2

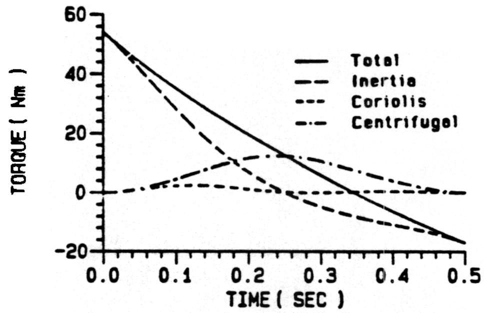

Motor for Joint 3

Figure 5: Torque Requirement on Each Actuator

SUMMARY AND FUTURE WORK

This paper presents some results of the on-going research project on statically-balanced direct drive arm at the University of Minnesota. The following features characterize this robot:

1. The statically-balanced mechanism without counterweights allows for selection of smaller actuators. Since in static or quasi-static operations, no load is on the actuators, therefore the overheating of the previous direct drive robots will be alleviated.

2. The robot links are being made of graphite-epoxy composite materials to give more structural stiffness and less mass. The high structural stiffness and low mass of the links allow for the wide bandwidth of the control system.

3. Electronic compliancy has been considered for control of the robot.

APPENDIX

A simple example is given here to show the that transmission system does not necessarily results in lower speed for the output shaft. Consider the following system:

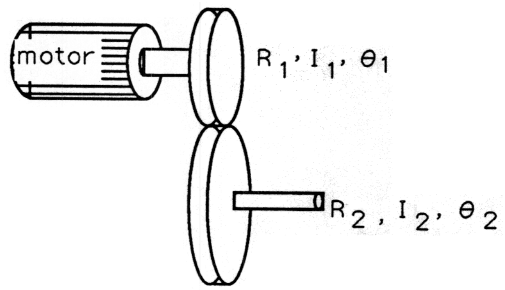

The dynamic equation describing the behavior of the system can be represented as:

$$\ddot{\theta}_2 = \frac{T}{(n I_1 + I_2/n)}$$

where (I_1, R_1, θ_1) and (I_2, R_2, θ_2) represent the moments of inertia, radius and angle of each gear ($n = R_2/R_1$). T is the motor torque. It is clear that the maximum acceleration will happen when n is chosen as:

$$n = \sqrt{I_2/I_1}$$

REFERENCES

Asada, H., Kanade, T., " Design of Direct Drive Mechanical arms", ASME Journal of Vibration, Acoustics, Stress, and Reliability in Design, vol. 105, July 1983, pp. 312 - 316

2 Asada, H., Kanade, K. and Takeyama, I., " A Direct-Drive Manipulator Developement of a High Speed Manipulator", in Brain, R. (compile), Development in Robotics 1984, Anchor Press, England, 1983, pp 217-226.

3 Asada, H., Youcef-Toumi, K. and Ramirez, R., "M. I. T. Direct Drive arm Project", Conference proceedings of Robots 8, vol.2, Robotics International of SME, 1984, pp 16-10 - 16-21.

4. Asada, H. and Youcef-Toumi, K., " Analysis and Design of a Direct Drive Arm with a Five-Bar-Link Parallel Drive Mechanism ", ASME Journal of Dynamic Systems, Measurement and Control, vol. 106 No. 3, 1984, pp 225-230.
5. Asada, H. and Slotine, J.-J.E., "Robot Analysis and Control", John Wiley and Sons, 1986.
6. Craig, J. J.., "Introduction to Robotics: Mechanics and Control, Addison-Wesley, Reading, Mass 1986.
7. Forrest-Barlach, M. G. and Babcock, S. M., "Inverse Dynamics Position Control of a Compliant Manipulator", IEEE 1986 International Conference on Robotics and Automation, vol 1 Apr. 1986, pp 196-205.
8. Hogan, N., "Impedance Control: An Approach to Manipulation, part 1: Theory, Part 2: Implementation, Part 3: Application", ASME Journal of Dynamic Systems, Measurement, and Control, 1985.
9. Houk, J. C., Rymer, W. Z., " Neural Control of Muscle Length and Tension", in Handbook of Physiology - The Nervous System II, pp257-323.
10. Kazerooni, H., Sheridan, T., B., Houpt, P. K., " Fundamentals of Robust Compliant Motion for Robot Manipulators" , IEEE Journal on Robotics and Automation, vol. 2, NO. 2, June 1986.
11. Kazerooni, H., Houpt, P. K., Sheridan, T., B., " Design Method for Robust Compliant Motion for Robot Manipulators" , IEEE Journal on Robotics and Automation, vol. 2, NO. 2, June 1986.
12. Kazerooni, H., Houpt, P. K., " On the Loop Transfer Recovery", International Journal of Control, vol. 43, NO. 3, March 1986.
13. Kuwahara, H., One, Y., Nikaido, M. and Matsumoto, T.," A Precision Direct Drive Robot Arm", Proceedings 85 American Control Conference, 1985, pp 722-727.
14. Mahalingam, S. and Sharan, A. M. "The Optimal Balancing of the Robotic Manipulators", IEEE 1986 International Conference on Robotics and Automation, vol. 2, April. 1986, pp 828-835.
15. Paul, R. P., Robot Manipulators: Mathematics, Programming, and Control", MIT press, Cambridge, Mass, 1981.
16. Rivin, E.I., "Effective Rigidity of Robot Structures: Analysis and Enhancement", Proceedings of 85 American Control Conference, 1985, pp 381-382.
17. Stein, R. B., " What muscle variable(s) does the Nervous System Control in Limb Movement?", The Behavioral and Brain Sciences, 1982, pp. 535 - 577.
18. Takase, K., Hasegawa, T. and Suehiro, T., "Design and Control of a Direct Drive Manipulator", Proceedings of the International Symposium on Design and Synthesis, Tokyo, Japan, July 1984, pp 347-352.